Analyzing Surgeon–Robot Cooperative Performance in Robot-Assisted Intravascular Catheterization

Wenjing Du, *Student Member, IEEE*, Guanlin Yi, Olatunji Mumini Omisore, *Senior Member, IEEE*, Wenke Duan, *Graduate Student Member, IEEE*, Toluwanimi Oluwadra Akinyemi, *Member, IEEE*, Xingyu Chen, Jiang Liu, *Senior Member, IEEE*, Boon-Giin Lee, *Senior Member, IEEE*, and Lei Wang, *Senior Member, IEEE*

***Abstract*—Robot-assisted catheterization offers a promising technique for cardiovascular interventions, addressing the limitations of manual interventional surgery, where precise tool manipulation is critical. In remote-control robotic systems, the lack of force feedback and imprecise navigation challenge cooperation between the surgeon and robot. This study proposes a manipulation-based evaluation framework to assess the cooperative performance between different operators and robot using kinesthetic, kinematic, and haptic data from multi-sensor technologies. The proposed evaluation framework achieves a recognition accuracy of 99.99% in assessing the cooperation between operator and robot. Additionally, the study investigates the impact of delay factors, considering no delay, constant delay, and variable delay, on cooperation characteristics. The findings suggest that variable delay contributes to improved cooperation performance between operator and robot in a primary-secondary isomorphic robotic system, compared to a constant delay factor. Furthermore, operators with experience in manual percutaneous coronary interventions exhibit significantly better cooperative manipulate on with the robot system than those without such experience, with respective synergy ratios of 89.66%, 90.28%, and 91.12% based on the three aspects of delay consideration. Moreover, the study explores interaction information, including distal force of tools-tissue and contact force of hand-control-ring, to understand how operators with different technical skills adjust their control strategy to prevent damage to the vascular vessel caused by excessive force while ensuring enough tension to navigate complex paths. The findings highlight the potential of variable delay to enhance cooperative control strategies in robotic catheterization systems, providing a basis for optimizing surgeon-robot collaboration in cardiovascular interventions.**

***Index Terms*—Cardiovascular interventions, cooperative manipulation, delay factor, interaction force, robot-assisted catheterization.**

Received 1 August 2023; revised 29 February 2024; accepted 27 August 2024. Date of publication 4 October 2024; date of current version 20 November 2024. This work was supported in part by the Natural Science Foundation of China under Grant U21A20480 and Grant U191320006; in part by the National Key R&D Program of China under Grant 2022YFC2409000; in part by Shenzhen Science and Technology Program under Grant JSGGKQTD20221101115654021; and in part by the Shenzhen Engineering Laboratory for Diagnosis and Treatment Key Technologies of Interventional Surgical Robots. This article was recommended by Associate Editor B. Hu. *(Corresponding authors: Boon-Giin Lee; Lei Wang.)*

This work involved human subjects in its research. Approval of all ethical and protocols was granted by Institutional Review Board (IRB) of the Shenzhen Institute of Advanced Technology (SIAT), Chinese Academy of Sciences under Application No. SIAT-IRB-220915-H0606.

Wenjing Du is with the Research Centre for Medical Robotics and Minimally Invasive Surgical Devices, Shenzhen Institutes of Advanced Technology, Chinese Academy of Sciences, Shenzhen 518055, China, and also with the Faculty of Science and Engineering, School of Computer Science, University of Nottingham Ningbo China, Ningbo 315104, China (e-mail: wj.du@siat.ac.cn).

Guanlin Yi, Olatunji Mumini Omisore, Toluwanimi Oluwadra Akinyemi, Xingyu Chen, and Lei Wang are with the Research Centre for Medical Robotics and Minimally Invasive Surgical Devices, Shenzhen Institutes of Advanced Technology, Chinese Academy of Sciences, Shenzhen 518055, China (e-mail: gl.yi@siat.ac.cn; omisore@siat.ac.cn; tolu@siat.ac.cn; xy.chen7@siat.ac.cn; wang.lei@siat.ac.cn).

Wenke Duan is with the Research Centre for Medical Robotics and Minimally Invasive Surgical Devices, Shenzhen Institutes of Advanced Technology, Chinese Academy of Sciences, Shenzhen 518055, China, and also with the Academy for Engineering and Technology, Fudan University, Shanghai 200437, China (e-mail: wk.duan@siat.ac.cn).

Jiang Liu is with the Department of Computer Science and Engineering, Southern University of Science and Technology, Shenzhen 518055, China (e-mail: liuj@sustech.edu.cn).

Boon-Giin Lee is with the Nottingham Ningbo China Beacons of Excellence Research and Innovation Institute, School of Computer Science, University of Nottingham Ningbo China, Ningbo 315100, China (e-mail: boon-giin.lee@nottingham.edu.cn).

This article has supplementary material provided by the authors and color versions of one or more figures available at https://doi.org/10.1109/THMS.2024.3452975.

Digital Object Identifier 10.1109/THMS.2024.3452975

I. Background Study

CARDIOVASCULAR diseases (CVDs) have emerged as the primary cause of mortality and disability-adjusted life worldwide [1], [2]. Despite global adoption, manual endovascular interventions are known with several challenges, such as the surgeons been faced with occupational risks, such as exposure to radiation from the X-ray fluoroscopy used for visualization, orthopedic injuries, and ergonomic fatigue [3], [4], [5].

In an effort to enhance operator comfort and minimize radiation exposure, there has been significant progress in the development of surgical robots for catheterization procedures. Notably, with the onset of the COVID-19 pandemic, teleoperated surgical robots have played a crucial role in reducing healthcare workers' exposure risk to the coronavirus [6]. During the mid-2000s, a number of robotic catheter systems (RCSs) were developed to address the challenges of manual endovascular interventions. Amongst the RCSs, which have achieved food and drug administration (FDA) approval and commercialization are the Niobe Magnetic Navigation System (Stereotaxis, Inc., USA), Amigo (Catheter Precision, USA), Sensei X (Hansen Medicals, USA), and CorPath 200 (Corindus Vascular Robotics, USA) [7]. The RCSs enable surgeons to operate remotely with the use of buttons, joysticks, or isomorphic primary interfaces [8], [9]. These have reduced the operational hazards interventionists experience during percutaneous coronary interventions (PCIs).

Although the advent of the remote-control interventional robotic system has shown remarkably good outcomes in the intravascular procedures, there are still unanswered existing

issues in robot-assisted cardiovascular interventions [10]. Due to the inherent design of the isomorphic primary–secondary interventional system, wherein a remote vascular intervention robot is divided into primary and secondary components, there will be a delay in the system's response. First, it is challenging to design collaborative control methods that engage intuition at both primary and secondary sides for endovascular tool navigation. Available studies on this have significant teleoperation latency and signal lagging [11]. Furthermore, modeling the interactive and operative forces between endovascular tool and patients' vessels has got very little success. These challenges hinder the developments in the subfield of human–robot cooperative control strategy, causing either surgeons or patients, and both in some cases, to be exposed to more risks during cardiovascular interventions. We articulate that these challenges can be further alleviated with primary–secondary systems built on intuitive architecture with human–machine synergy. In scenarios for efficient tool manipulation completion, tactic coordination of the interventionalists and RCS is vital [12].

Several factors, such as communication delays, RCS dynamics, and surgeons' tool manipulation skills, require further studies. Smirnov and Ponomarev [13] proposed a concept of cooperation index to coordinate human–machine intelligence for collaborative robot-assisted intervention. However, the efficiency of the primary–secondary operation is affected by the network transmission time, packet transmission rates, and bandwidth limitations. The study shows that time delay affecting primary–secondary operations might be unavoidable. Thus, it may be more practical to focus on developing event-driven instead of time-driven frameworks. This will guarantee seamless primary–secondary operation in RCSs [14], [15]. Xi et al. [16] motivated the development of an event-driven approach for effective primary–secondary RCS operation. In another study, it was shown that combining event-based robotic autonomy or intelligence with human cognition can effectively improve tool manipulation in an RCS setup [17]. This can open new study directions, such as the development of manipulation-driven systems in robot-assisted intravascular interventions. As a new approach, modeling manipulation-based framework can offer novel ways of evaluating the collective performance, such as surgeon–robot manipulation indices of interventionalists and robotic system during robot-assisted catheterization.

Exception for considering the influence of communication delays on human–machine synergy performance, interaction force, such as the application of an excessive force, could affect cooperation performance between the operator and robotic system. The major issue in the available primary–secondary intervention surgical systems is the lack of reliable haptic feedback, leaving surgeons to only rely on their visual sensing during the procedure. Operators face challenges in real-time perception of distal and proximal force, leading to sudden variations in haptic force, manipulating speed, or changes in behavior models due to different technical skills. As a consequence, the robotic system may not promptly adapt and respond to the surgeon's operational commands, resulting in suboptimal cooperation performance between the operator and the robot. Therefore, this requires extensive knowledge about the dynamics of the surgical robots and endovascular tools, tool motion tracking and analysis, interaction of the tools with patient's blood vessels, and interventionalists' manipulation behavior. Huang et al. [18] presented a comprehensive study on recent developments in modeling tool–tissue interaction. Similarly, Reiley and Hager [19] proposed using interaction force and motion between tools and vessels for assessing interventionalists' catheterization skills. Zhou et al. [20] proposed a behavior-based assessment framework to utilize interventionalists' catheterization behaviors proxy on their hand movement, proximal strength, muscle activity, and finger movement to assess their tool catheterization skills. Also, Du et al. [21] developed a model that uses interventionalists' kinematics, kinesthesis, and robot's motion data to explore the potential of integrating surgeons' operational skills into robot-assisted PCI. Studies from Patel et al.'s article [22] show that adding operational force, such as tactile or haptics information, present to optimize the minimally invasive interventions. While integrating tool–vessel force has received sufficient attention, Gao [23] et al. developed magnetorheological fluid technology for haptics feedback in the primary interface of an RCS. Also, Gan et al. [24] designed a fiber-optic-based for distal force sensing and deployed it for measuring interaction force from the tip of catheter during minimally invasive interventions. This can aid robot-assisted percutaneous coronary intervention (R-PCI) by providing tactile and haptics feedback to interventionalist.

It is important to note that, whereas the time-based communication delays mentioned models and tool–tissue interaction approaches of technical skill may differ from each other fundamentally, it is not only their validity that should be considered, but their applicability for the specific task that should also be considered when choosing the right model for a given problem. In order to improve the cooperation performance between operators and the primary–secondary isomorphic robotic system in robot-assisted interventional applications, a manipulation-based evaluation framework is proposed and developed. This framework aims to assess the cooperation performance between operators and the robotic system during robot-assisted cardiovascular interventions, ultimately enhancing the application and development of robot-assisted intervention techniques. The primary contributions of this study are outlined as follows.

1) Development of a manipulation-based machine-learning framework designed to analyze the synergy performance between operators and the robot. The proposed framework, utilizing the synergy ratio, demonstrates excellent performance in assessing the cooperative manipulation between operators and the robot.
2) Investigation of the impact of delay factors on the synergy ratio between human and robot from three perspectives, namely, no delay, constant delay, and variable delay. This analysis validates the potential benefits of employing manipulation-based variable delay to enhance the cooperative control strategy for the primary–secondary isomorphic robotic system.
3) Analysis of interaction forces, such as distal force and haptic force, concerning complex vascular paths. This analysis offers insights into how operators with different technical skills adjust their control strategies to avoid causing damage to vascular vessels due to excessive force while still providing sufficient tension to navigate complex paths. This exploration significantly contributes to skill assessment in robot-assisted interventional surgery.

This study was carried out with the prototype of an isomorphic primary–secondary RCS that has been described in our previous studies [25], [26], [27]. As shown in Fig. 1, the robotic system is made of different components, such as the primary and secondary robotic devices, which share an isomorphic

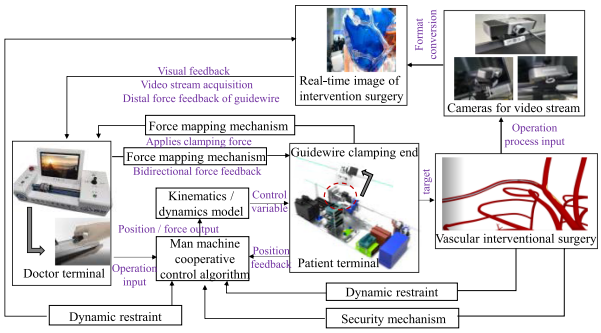

Fig. 1. View of the primary–secondary robot designed for intravascular interventions.

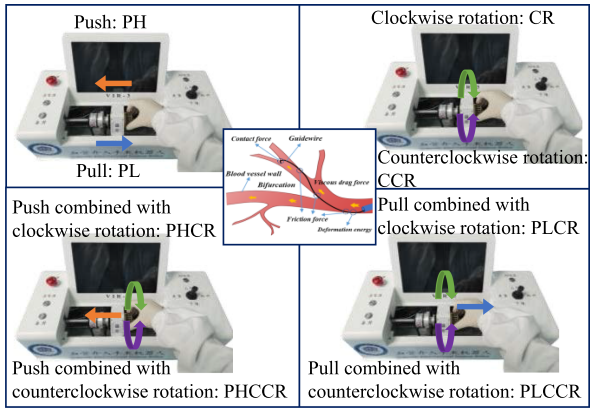

Fig. 2. Nine types of manipulating patterns during robot-assisted interventional surgery in the vascular simulator.

design that allows the interventionalists to exhibit the hand-defter capabilities used for cardiovascular catheterization during CVD interventions. The RCS is augmented with additional external devices for the acquisition of interventionalists' kinesthesis, kinematics, and haptics data. This information is, respectively, obtained with surface electromyography (sEMG) electrodes, electromagnetic sensors and fiber-optic glove, and flexible haptic sensor all worn by interventionalists during catheterization in R-PCIs. In addition, the kinematics of the secondary robot is obtained proximally with commercial sensor and distally through medical image processing, respectively. The primary objective of this study is to evaluate the synergy characteristics between human and robot during robot-assisted catheterization in R-PCIs. To achieve this, a synergy performance framework is proposed and developed, incorporating multiple data sources and the analysis of tool interaction data.

II. System Design and Methodology

A. Platform of Robot-Assisted Intravascular Interventions

Obtaining various signals during the catheterization procedure is crucial for studying the synergy performance between the operator and the robot in robot-assisted cardiovascular interventions. To achieve this objective, we utilized multisensor technologies to capture multimodal data, including video streams, time-series signals, robotic motion information, and interaction forces, during successful robot-assisted catheterization procedures. These data were acquired using our developed primary–secondary isomorphic RCS platform, as depicted in Fig. 3. The RCS capable of primary–secondary teleoperation with multiple degree-of-freedom (DoF) motions is used for intravascular catheterization in emulated R-PCIs. The RCS has a smart grasper that can change the orientation of clamped endovascular tools (such as the guidewire or catheter) and sense tool operational force during the R-PCIs. Also, the RCS was equipped with potentiometer sensor for decoding control signals and transmitting to secondary robot in real time. The RCS can implement all hand motions' (HMs) interventionists used for tool navigation during intravascular interventions. By comparison with the third-generation RCS [25], the improved prototype of the RCS logs proximal and distal force. Also, a 32-channel flexible tactile sensor was designed and attached for acquiring tactile force between the interventionalist's hand and the sleeve during intravascular interventions. Finally, the improved prototype also includes a proximal sensor attached to the secondary robot's slider for obtaining frictional force resulting from intravascular resistance. This configuration enables the acquisition of multiple signals during R-PCIs, facilitating the investigation of synergy manipulation characteristics between the operator and the primary–secondary isomorphic robotic system.

B. Phantom-Based Cardiovascular Path Modeling

In order to enhance the realism of the vascular environment simulation, a 1:1 ratio adult vascular simulator was utilized, replicating the actual vascular path. The steps followed in clinical practice were emulated by introducing guidewire through the lumen of a guiding catheter into the anterior descending branch of the phantom. The vessel path was filled with blood-like fluid that flows in real time with the aid of a cycling pump connected to the vascular phantom. Each procedure required the subjects catheterizing the endovascular tool (i.e., guidewire) from a starting point to a desired point (target). In this study, a total of 168 robot-assisted trials were completed, which includes exactly 12 trials per subject. In all cases, the operators were preinformed about the chosen vascular path by using visual analysis from a prerecorded video stream.

Studies started with path creation in which a guide catheter was inserted via femoral artery along vessel to coronary arteries ostia in simulator and introducer guidewire via coronary arteries ostia vessel along the anterior descending branch to target point, as shown in Fig. 3(e). This path consisted of one branch (part A), two stenoses (parts B and C rated as 37.45% and 42.69%, respectively), and tortuous routes (part D).

C. HMs Used for Guidewire Delivery

During robot-assisted catheterization, the RCS facilitates the control of flexible endovascular tools (such as guidewires or catheters) with axial translational movement, radial rotational movement, and compound movement. Generally, the operator delivers the guidewire or catheter using nine HMs to direct the RCS for guidewire delivery. These include pulling action and axial retraction (i.e., *Pull* [PL] and *Push* [PH]), radial rotation (*Clockwise Rotation* [CR] and *Counterclockwise Rotation* [CCR]), compound axial–radial motion (*Clockwise Rotation with Push* [PHCR], *Clockwise Rotation with Pull* [PLCR],

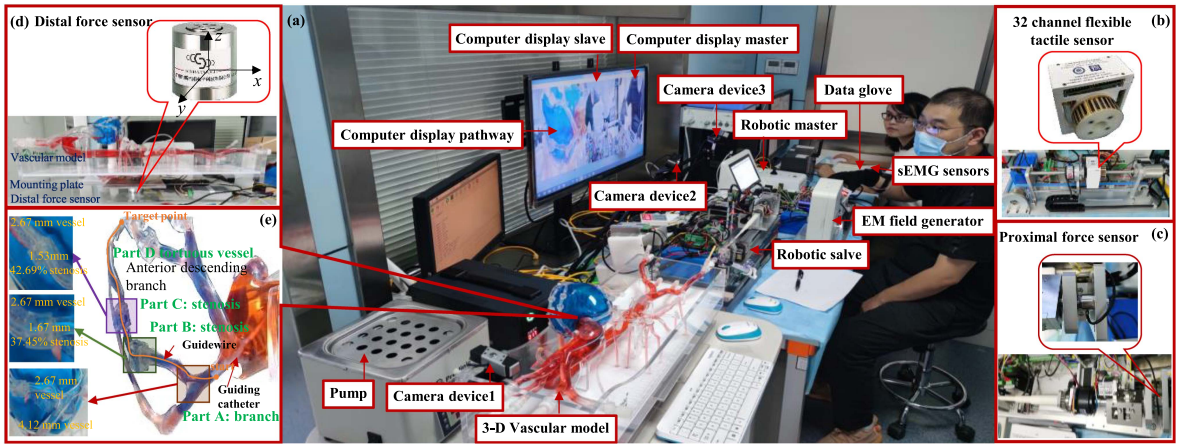

Fig. 3. Experimental setup showing the (a)–(e) original data collected from the portrait of the experiment setup in vascular simulator, and (a) display the whole system platform, (b) and (c) represent the haptic, proximal, and distal force sensors, respectively; (e) show the motion pathway of guidewire delivery from start point (orange color) to target point (orange color).

Counterclockwise Rotation with Push [PHCCR], *Counterclockwise Rotation with Pull* [PLCCR]), and static stage [SS], as presented in Fig. 2.

D. Decoding Operators' Catheterization Behaviors

By preforming intravascular catheterization in the simulator with the primary–secondary RCS in Fig. 3, operators' catheterization behaviors were obtained. The catheterization behaviors were characterized by operators' hand kinesthesis and kinematics data when completing the robot-assisted task. For quantifying the robot's contribution, low-order motion data (i.e., position and orientation) from the video stream of guidewire angiograms, the operational force from distal and proximal parts of the RCS, and haptic force received at the operator's side were also obtained. The surgeon-side and robot-side data were multiplexed for developing manipulation-based evaluation model for human–machine synergy assessment. Each session starts with a short tutorial wherein the operators are informed about the experimental procedure and given a signed informed consent form. The operators were allowed to complete the task independently. For data consistency, the guidewire is prepared to start at a similar position during each experimental session. Thus, the operators started the manipulation in a unique mode.

The dataset obtained from the 168 trials comprises 58 channel signals, including 4 channels for EMG data of muscle activities (MAs), 14-channel glove data for HM, 3-channel data from distal force for interaction information of vascular tool–tissue, 1-channel force data from the tool-robotic instrument, 32-channel haptic force for hand–control ring, and 4 channels for position and rotation information. These various data sources are utilized to assess the synergy characteristics between the operator and the robot. For further details regarding the devices used for each data source, refer to Appendix A (see Section II–D and Table I).

1) sEMG Signal Acquisition of Interested Muscle Activity: Typically, sEMG signals are utilized to capture neuromuscular activity during the movement of upper and lower limb parts in the human body. However, these conventional sEMG signals are primarily designed for noninvasive acquisition of physiological signals that trigger limb movements. In our study, we specifically acquired sEMG signals to characterize the muscle activity of the interventionists' hand and arm. To accomplish this, we used a commercial multichannel wireless EMG system (BIOPAC Systems, Inc., Goleta, CA, USA) to capture the muscle activity signals of the operators' right hand and right arm at a sampling rate of 2000 Hz. The simultaneously acquired sEMG signals included those from the abductor pollicis brevis, flexor carpi radialis, dorsal interossei, and extensor carpi radialis muscles. To ensure high signal quality, the skin of the operator was properly cleaned with alcohol prior to each experimental session, and the center-to-center distance between the electrodes of each channel was made less than 20 mm. In each experimental trial, the operator utilized the interventional robot to deliver the guidewire from point A to target point B. Consequently, signals associated with each muscle motion were acquired and saved separately for further processing.

TABLE I
DELIVERY SPEED AMONG THREE DIFFERENT GROUPS

Manipulation speed(mm/s)	Primary			Secondary		
	A_A	A_B	B	A_A	A_B	B
PH	53.65	55.69	51.32	52.99	54.51	51.57
PL	53.33	57.31	54.03	54.18	57.97	54.45
CR	299.05	135.41	117.67	107.89	122.63	105.27
CCR	581.83	275.19	107.83	314.22	118.49	97.39
PHCR	114.58	108.25	108.22	123.19	107.48	91.77
PLCR	88.69	82.73	111.09	81.59	87.24	103.16
PHCCR	88.91	93.19	205.68	239.58	75.69	146.93
PLCCR	65.42	77.15	91.59	132.14	74.19	91.59

2) Glove Signal Acquisition of HM: During the intervention, the interventionists employed axial translational movement, radial rotational movement, and compound movement to deliver the guidewire, resulting in distinct movement patterns of their hands. To capture these data, a fiber-optic glove, specifically the Data Glove 14 Ultra (Fifth Dimension Technologies, Suite Orlando, FL, USA) was used to obtain information on the bending of the operators' fingers. The HM data include flexure of the fingers and the abduction between them. Thus, 14-channel signals from thumb near (*tn*), thumb far (*tf*), thumb/index (*ti*), index near (*in*), index far (*if*), index/middle (*im*), middle near (*mn*), middle far (*mf*), middle/ring (*mr*), ring near (*rn*), ring far (*rf*), ring/little (*rl*), little near (*ln*), and little far(*lf*) were gotten at a fixed rate of 60 Hz. The values acquired are adopted as the displacement information of HM and used to build the

evaluation framework of human–machine synergy performance during robot-assisted intravascular interventions.

3) Acquisition of Distal Tool–Tissue Operational Force: In typical vascular interventional procedures, 2-D real-time fluoroscopy is the primary method for visual guidance in endovascular interventions. However, in cases where physicians lack 3-D anatomical information of blood vessels, force feedback becomes crucial for the interventionists. This is especially true for remote vascular intervention robots, where the interaction force between instruments and tissues cannot be perceived, increasing the risk of thrombosis and vascular perforation due to excessive force during surgery [28]. To directly measure the contact force between the instrument and tissue during guidewire delivery, a distal force-sensing platform was designed. This platform consists of a silicone-based anthropomorphic vascular model mounted onto a plate and rigidly coupled to a 6-DoF F/T sensor (SBT308, SIMBATOUCH, Guangzhou, China), with a composite error of 1.0% for the sensor. The sensor was mounted close to the platform's center of gravity, and the sensor provides force reading in each of the three (x, y, and z) directions, the maximum measurement range of three directions is all 49N, and sensitivity is x-1.038093 mV/V, y-1.03985 mV/V, and z-0.97937 mV/V, respectively, as shown in Fig. 3(d).

4) Acquisition of Proximal Robot-Tool Operational Force: The proximal force is a combination of the interaction force between the tool and tissue, as well as the friction force between the robot device and the tool held during robot-assisted intervention procedures. This proximal force can serve as an indirect measurement method to assess the interaction force between tools and tissue in the blood vessel. To achieve this, we developed a point contact proximal sensing platform to obtain the proximal force information, as illustrated in Fig. 3(c). The proximal force sensor (SBT674-2kg, SIMBATOUCH) is coupled to a robotic secondary mechanical assembly that measures axial (pull/push) loads. The maximum measurement range of the proximal force sensor is 19.6 N, and the sensitivity is $1.0 \pm 10\%$ mV/V, and the sensor provides force reading in one (z) direction. When the flexible endovascular tool (guidewire) is clamped in the secondary robot, and forward motion is issued along vascular path, the force sensor records the operational forces in real time.

5) Contact Force Acquisition in Fingers–Control Ring: During manual PCI procedures, the interventionist directly exerts a contact force on the catheter/guidewire, relying on various visual guidance and haptic cues to adjust their manipulation strategy for safely reaching the lesion location. However, this dynamic changes in robot-assisted PCI procedures, as robotic systems lack the capability to provide surgeons with sufficient haptic data sensory. To address this limitation, we designed a pressure measurement device with a multichannel flexible pressure sensor to be attached to the control ring of the primary robotic device. This device enables the acquisition of haptic force data between the finger and control ring. For detailed information about the design of the pressure measurement device, refer to Appendix A (see Section II–D5) *titled "Operator's Contact Force…."* The 32-channel flexible pressure sensor used in this setup has a sensitive area size of $2*12$ mm and a force range from 0.01 to 19.6N. These haptic force data are essential for understanding the forces applied by operators to guide the tip motion of the endovascular tool during robot-assisted catheterization and for assessing the performance of the tool by both the surgeon and the robot.

6) Video Stream Data Acquisition: To document the robot-assisted intervention procedure, three cameras were utilized for distinct purposes. The first camera recorded the operators' HMs while manipulating the primary robotic device, providing a comprehensive view of their catheterization maneuvers along the paths, as depicted in Fig. 3. The video data from this camera, acquired at a frame rate of 30 frames per second, captured the operator's behavior and their manipulation of the robotic primary mechanism. The second camera was dedicated to capturing the motion procedure of the held guidewire delivery from the secondary robotic device. It depicted how the secondary device executed actions in response to commands received from the primary device. This camera's footage offered valuable insights into the coordination between the primary and secondary robotic components. Finally, the third camera was specifically utilized for offline video analysis. It allowed for the identification and annotation of pathological segments within the video frames, including part A: branch, part B: stenosis, part C: stenosis, and part D: tortuous path. This analysis helped in understanding and evaluating the effectiveness of the robot-assisted intervention procedure in handling different challenging scenarios.

E. Signal Processing and Technical Skill Division

1) Signal Processing: Operators are given the task of catheterizing guidewire from the coronary ostium (start point) to target point (the ending anterior descending branch). The data from the multiple data sources are saved separately used processed further as described in the following text.

a) Data preprocessing: The sEMG signal is a nonstationary microelectrical signal characterized by an amplitude range of 0–1.5 mV and a useful signal frequency range of 0–500 Hz. To enhance the signal quality, a 10–500 Hz bandpass filter was applied to eliminate any components outside the desired frequency bandwidth. Additionally, a 50-Hz notch filter was employed to eliminate power frequency disturbances. To ensure uniformity across different operators in the sEMG dataset, we utilized minimum and maximum normalization functions to normalize the sEMG signal. This normalization ensured a fair comparison between signals acquired from all operators. For the remaining data obtained from glove data of HM, distal and proximal interaction force, haptic force, and position and rotation displacement of the primary–secondary system, we applied smoothing processing using an average filter. This step effectively removed any abnormal data and spikes in the motion, resulting in a more reliable and consistent dataset for further analysis.

b) Resampling: The sampling rates of the different signals in the setup vary; the sEMG signals have a sampling rate of 2000 Hz, and that is higher than that of finger motion (60 Hz), position and rotation data in the RCS, tool–vessel distal force (60 Hz), the haptic force signal (50 Hz), and proximal force of tool instrument (100 Hz), respectively. These acquired sequences are not matched in time domain. To ensure that the signals align when used for developing the proposed learning-based system, the high-frequency signals are synchronously processed with low-frequency according to timestamp.

2) Division of Operators' Technical Skill: A total of 14 operators were recruited from the University of Chinese Academy

of Sciences Shenzhen Hospital and Shenzhen Institutes of Advanced Technology in Shenzhen, China. The operators participating in the study were categorized into two groups: group A, comprising ten subjects with no prior M-PCI experience, and group B, which consisted of five subjects with M-PCI experience. Within group A, further division was performed using the k-means clustering method based on the time spent in cannulating the vascular pathway and the number of robot-assisted interventional procedure training sessions on the vascular simulator. This division resulted in two subgroups: group A_A, with operators showing longer manipulation time and fewer training sessions in robot-assisted PCI vascular simulator procedures, and group A_B, with operators displaying shorter manipulation time and more training sessions in robot-assisted PCI vascular simulator procedures. Consequently, group A_A, group A_B, and group B represented different technical skill levels, which were defined as level A, level B, and level C, respectively. For more details about the operator division, refer to *Fig. A2* in Appendix A (see Section II–E2) *titled "The Division of Operators…."*

III. Evaluation Framework Based on Manipulation

In this study, a convolutional neural network (CNN) based evaluation framework was proposed to assess the synergy characteristic between different technical skill operators and the robot. The framework incorporates convolutional and dense layers and utilizes an attention block to capture relevant gradients from multimodal data. The choice of a CNN model was made due to its efficient learning capabilities within a simplified network structure.

The evaluation framework comprises three stages:

1) signal acquisition and data processing;
2) feature extraction using a CNN model;
3) manipulation pattern recognition based on a fully connected network.

The process of data acquisition and preprocessing is described in Section II. The CNN model used for feature extraction consists of three types of layers:

1) an input layer with units L_i^0, where the input dataset has fixed values;
2) hidden layers with units L_i^m, where the values are derived from the previous layers (m–1);
3) an output layer with units L_i^M, where the values are derived from the last hidden layer.

The model adjusted a set of weights $w_{i,j}^m$ to learn, where $w_{i,j}^m$ represents the weight from an input L_i^m to an output unit L_j^{m+1}. The total input is denoted as (6, X_i^m), and Y_i^m represents the output of unit L_i^m.

In the proposed framework, the preprocessed dataset was input into the CNN-attention module, which extracted deep features from high-dimensional data consisting of 58 channels. These channels include 4 channels from sEMG data of muscle activity, 14 channels from finger flexion of HM, 32 channels of contact force, 1 channel of proximal force, 3 channels of distal force, and 4 channels of position and rotation displacement information from the primary–secondary robotic system. These channels are organized into matrices of dimension (6, X_i^m), and then fed into the CNN module. Next, deep feature vectors (F) are extracted from each chunk by segmenting the data using a unique sliding window approach with window sizes of $6 \times C \times S$. This segmentation approach is employed to reduce the impact of transiency and randomness in nonstationary signals. The window properties are chosen carefully to ensure that most segments cover complete cycles of each motion type during the robot-assisted guidewire delivery procedure. As a result, each segment contains unit hand movements performed by each surgeon and is organized as a matrix, with C representing the number of channels and S representing the number of segments used.

Fig. 4 depicts the CNN component, which comprises a variable number ($n = 2, 3, \ldots, N$) of convolutional blocks. Each block includes a single convolution layer with 32 or 64 kernels of size 1, a stride of 1, and padding of 1, utilized for feature extraction, resulting in multidimensional feature maps. To optimize model performance by eliminating redundant features, a CNN-attention network is introduced to operate on both local and global feature maps. The channel attention module is utilized to extract salient features by learning the characteristics of the multidimensional time series. The initial feature maps are processed through a convolutional layer with max pooling, pooling the features in the channel direction using a kernel size of 1, a stride of 1, and no padding. Subsequently, the feature maps are fed into a convolutional layer using average pooling to pool the features. The resulting feature maps are considered as vector-level local features, and the salient features are recalculated using a weight vector. To enhance the overall performance and obtain deep information, a spatial attention module is employed to capture global information.

This module consists of one max-pooling operation, one average-pooling operation, one sigmoid operation, and four convolution operations. The sigmoid function is used to constrain the output range between 0 and 1, where 0 indicates an irrelevant patch and 1 denotes the highly important feature patch. The procedure transforms the feature maps into a vector of global feature. The process is repeated two times to obtain the feature maps. Finally, the extracted features are fed into a SoftMax logistic module for manipulation pattern recognition, enabling the framework to recognize and categorize different manipulation patterns effectively.

A. Training Strategy

The categorical cross-entropy loss function is used by the network, which is defined as follows:

$$\text{Loss} = -\sum_{i=1}^{n} \hat{y}_{i1}\log y_{i1} + \hat{y}_{i2}\log y_{i2} + L + \hat{y}_{im}\log y_{im} \quad (1)$$

where n is the number of samples, m is the number of classification and $m > 2$, $\hat{y}_{im}$ has the value of 1 when the sample belongs to category m; otherwise, it is 0 and y_{im} represents the probability that sample is predicted to be class m. The total of 348 760 samples is partitioned into 70% (244 132), 10% (34 876), and 20% (69 752) for the network training, validation, and testing, respectively. The deep learning optimizer of Adam is selected, which is defined in (2). It turns out that the following deep learning network iterates fast:

$$Ffs = \frac{1}{n}\sum_{i}^{n}\frac{1}{t_i}. \quad (2)$$

The network underwent training for 100 epochs, and its performance was assessed using various validation metrics. Throughout the training process, the model's parameters were dynamically modified as the multimodal data flowed through the network, ensuring adaptability to the dataset. Training continued until the loss value ceased to decrease. The flowchart of the proposed framework training is illustrated in Fig. 5.

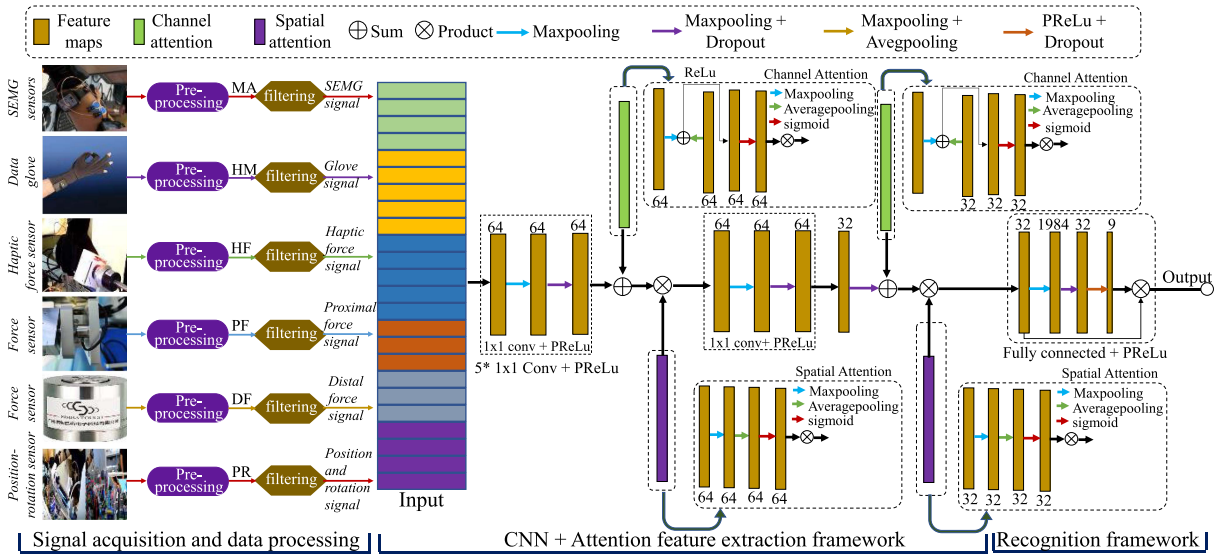

Fig. 4. Evaluation framework of surgeon–robot synergy performance during robot-assisted intravascular interventional surgery.

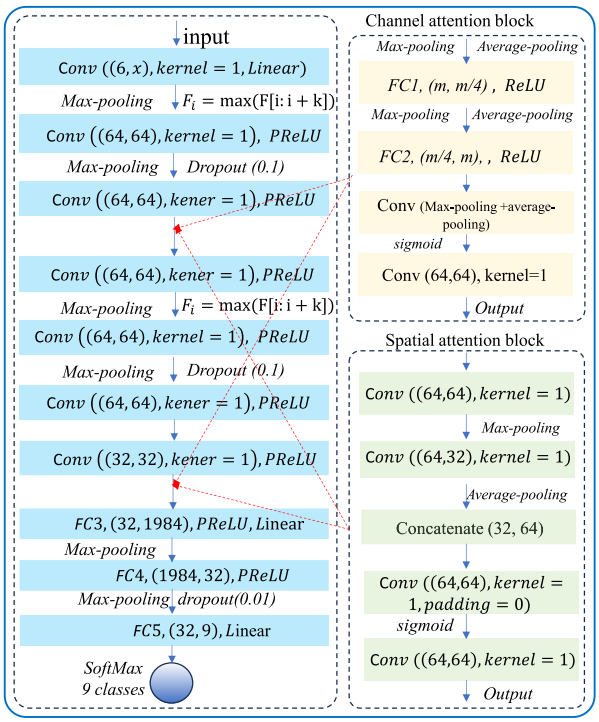

Fig. 5. Flowchart of the model training.

This study's primary objective is to analyze the synergy characteristic between humans and robots in a primary–secondary isomorphic robotic system. Consequently, it can be viewed as a nine-class manipulation classification task. Model performance was evaluated based on precision (Pre), recall (Rec), and accuracy (Acc), which were calculated, as shown in (3), (4), and (5) respectively

$$\mathrm{Pre} = \mathrm{TP}/(\mathrm{TP}+\mathrm{FP}) \tag{3}$$

$$\mathrm{Rec} = \mathrm{TP}/(\mathrm{TP}+\mathrm{FN}) \tag{4}$$

$$\mathrm{Acc} = (\mathrm{TP}+\mathrm{TN})/(\mathrm{TP}+\mathrm{FP}+\mathrm{TN}+\mathrm{FN}) \tag{5}$$

where TP, TN, FP, and FN represent the true position, true negative, false positive, and false negative, respectively. The model with 0.0002 learning rate obtained the highest accuracy on training and validation dataset as final model to evaluate the synergy performance on testing dataset, as shown in Appendix A (see Section III–A and Fig. A3). At this point, a tenfold was applied in training procedure; we obtained a well-trained model with the average training accuracy of 99.50 ± 0.16% and validation accuracy of 99.85 ± 0.20%, respectively. These results show that the extracted features would be a better basis for the proposed synergy framework to evaluate human–robot coordination performance.

B. Human–Machine Synergy Evaluation Strategy

To explore the synergy performance between the operator and the primary–secondary isomorphic robotic system, we applied the proposed framework to assess the synergy of the robot system and improve its coordination. Since the operator directly manipulates the primary robotic device, their motion pattern is considered as Label A∈(PH, PL, CR, CCR, PHCR, PLCR, PHCCR, and PLCCR). Subsequently, the secondary robotic device replicates the operator's motion command to manipulate the interventional tools, and the motion pattern of manipulating the interventional tools is regarded as Label B∈(PH, PL, CR, CCR, PHCR, PLCR, PHCCR, and PLCCR). If the secondary robotic device follows the motion pattern of the operator's manipulation of the primary robot effectively, it indicates good cooperation between the human and the robot. Conversely, if the secondary robot's motion pattern becomes more random, it suggests poor cooperation between the human and the robot.

Therefore, the proposed evaluation framework achieves high accuracy ($\mathrm{Acc}_{\mathrm{primary}}$) in recognizing the manipulation pattern of the primary device when the cooperation between operators and the robot is good, and also obtains high accuracy ($\mathrm{Acc}_{\mathrm{secondary}}$) in recognizing the motion pattern of the secondary device. Conversely, in the case of poor cooperation between operator and robot, the framework achieves high accuracy in recognizing the manipulation pattern of the primary device but low accuracy in recognizing the motion pattern of the secondary device. The synergy ratio is then used to denote the synergy performance between operator and robot, which can be explained as follows:

$$\mathrm{SynergyRatio} = (\mathrm{Acc}_{\mathrm{primary}} \times \mathrm{Acc}_{\mathrm{secondary}}) \times 100\%. \tag{6}$$

A higher synergy ratio (closer to 1) indicates better cooperation between the operator and the robot, while a lower synergy ratio (closer to 0) suggests poor cooperation.

To capture the motion of the operator's hand manipulation, a magnetostrictive position sensor (SDM20T-0150-MR2P-MEP03-1, Soway Tech., Shenzhen, China) and a rotary encoder (E40H12-1000-3-N-5, Autonics, Busan, South Korea) are used to measure axial position and rotation motion, respectively. The handle operated by the operator consists of a hollow magnetic ring, a hollow rotary encoder, and a bracket connected to the slider, enabling simultaneous rotational and axial movements while preserving the operator's natural catheterization skills. The detailed design specifications of the linear or rotary motors for the axial or rotary drive from the secondary device were extensively covered in our previous publication [29].

For teleoperating robotic systems, a key factor in human–robot synergy is whether the secondary executing device can promptly and accurately complete the motion pattern of the operator's manipulation of the primary robot. Delays in the robotic system can lead to lower synergy ratios between the operator and the robot. Therefore, we considered three aspects to assess the synergy ratio between the operator and the primary–secondary isomorphic teleoperation system. First, under the assumption of no delay in the current primary–secondary isomorphic robotic system, the evaluation framework was applied to assess the cooperation between the operator and the robot. Second, considering a constant parameter (0.254 s) based on the communication delay of the system to assess the synergy ratio between the operator and the robot. Finally, considering the variable delay based on the manipulation pattern to obtain the synergy ratio between the operator and the robot. This approach helps us understand the system's real delay characteristic and allows us to optimize the cooperation strategy for improved performance.

IV. Cooperative Performance and Analysis of Interaction Information

In this section, we analyze the cooperative performance between humans and machines, considering three key aspects: no-delay, constant-delay, and variable-delay factors. The goal is to enhance the cooperative performance between operators with varying technical skills and the robotic system, ultimately improving the safety and effectiveness of the robotic system during robot-assisted PCI procedures. Additionally, we analyze the contact force between the hand and instrument, as well as the distal force between the intravascular tool and tissue, to understand how different technical skill operators adjust their control strategies to ensure that they do not cause damage to the vascular vessel through excessive force while navigating complex paths. To achieve this, we utilized multiple data sources to build the proposed framework for assessing the cooperative performance between operators and the robotic system. We tested the framework using a separate dataset to verify its performance. Subsequently, we analyzed the cooperative performance between different technical skill operators and the robot, considering three aspects:

1) no-delay factor between operator and robot;
2) existing constant communication-delay factor;
3) existing variable-delay factor based on manipulation patterns.

Finally, we employed the Kruskal–Wallis analysis of variance (ANOVA) statistical method to analyze the significant differences in manipulation time, haptic force, and distal force among the three different technical skill operators during robot-assisted guidewire delivery through branch vessels, stenosis vessels, and tortuous vessel paths, respectively.

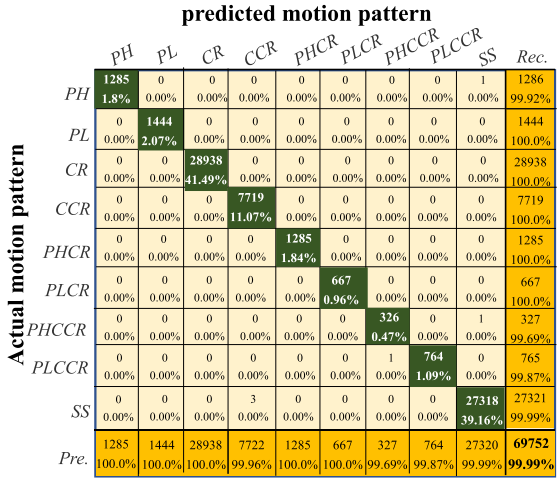

Fig. 6. Performance of the proposed framework on the testing set.

A. Analysis of the Cooperative Performance Between Operator and Robot

Since the evaluation framework was built based on multiple data sources, and the target function of model training is based on the manipulation pattern of primary device, the premise that the framework can be used as an evaluation role to assess cooperative performance between human and robot is the performance of the prediction primary device's motion pattern, which is good enough with a very few occasional false negatives or false positives. If the performance of framework on primary's motion pattern is poor, this framework does little to assess the output prediction results on cooperative performance between human and machine. Therefore, the reliability of results of cooperative performance between human and machine relied on the good prediction results of framework on primary motion pattern. The performance of the proposed model is evaluated using accuracy, recall, and precision values. The result showed that the model obtained high accuracies of 99.99% on the test dataset, while the precision accuracy based on each motion pattern was also high with PH-100%, PL-100%, CR-100%, CCR-99.96%, PHCR-100%, PLCR-100%, PHCCR-99.96%, PLCCR-99.87%, and SS-99.99% in Fig. 6, respectively.

Based on the above high-accuracy model, to demonstrate the cooperative performance between different technical skill operators and robot on three different delay factors consideration during robot-assisted PCI procedure, the synergy ratio between operator and robot was shown in Fig. 7. The results showed that the synergy ratio based on no-delay factor was 49.84% (A_A), 51.84% (A_B), and 53.42% (B) among three group operators with different technical skills in Fig. 7(a), respectively, which suggested that the current primary–secondary isomorphic robotic system exists some delay factor. Similarly, based on a constant communication-delay factor consideration, the results suggested the synergy ratio of 51.88% between operator A_A and robot, 56.17% between operator A_B and robot, and 58.71% between operator B and robot, which seems to slightly increase compared with synergy ratio based on no-delay factor. The obtained results revealed that the cooperative performance between the operator

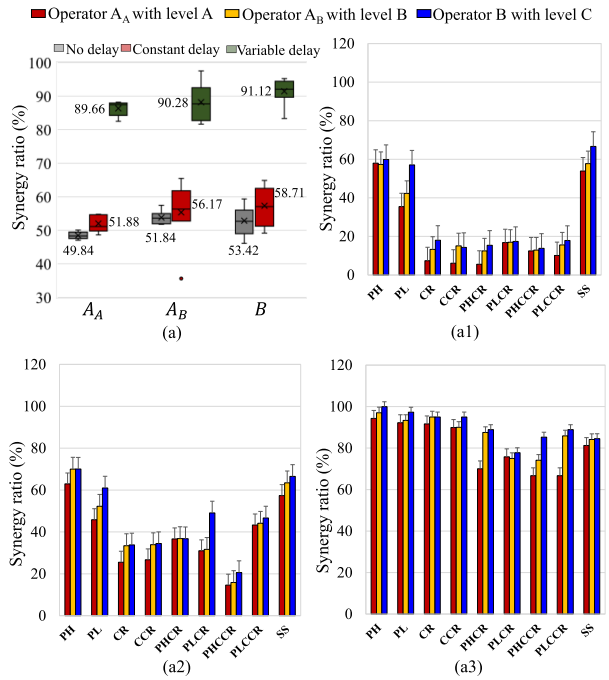

Fig. 7. Performance of surgeon–robot synergy in operator with three different skill levels, (a) synergy ratio based on three different delay factors, (a1) no delay, (a2) constant delay, and (a3) variable delay.

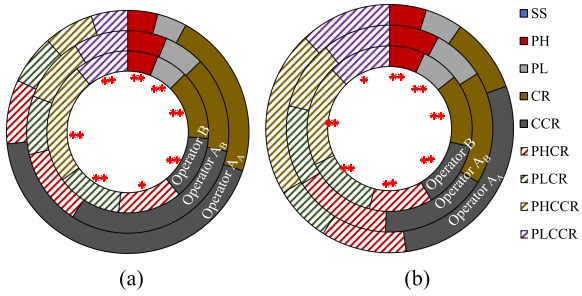

Fig. 8. Manipulating speed of robot primary and secondary mechanism based on different movement patterns, the speed of (a) robotic primary and (b) robotic secondary. $*$: significant difference ($*$: at 0.05 level, and $**$: at 0.01 level). (a) Speed in primary device. (b) Speed in secondary device.

and the robot is influenced by additional delay factors beyond the constant delay factor considered. Subsequently, when considering the variable-delay factor based on the manipulation pattern, the synergy ratio was found to be 89.66% between operator A_A and the robot, 90.28% between operator A_B and the robot, and 91.12% between operator B and the robot. These results indicate that the variable-delay factor significantly enhances the cooperation performance between the operator and the primary–secondary isomorphic robotic system when compared with the constant delay factor.

Furthermore, the study delved deeper into the synergy ratio of different manipulation patterns, considering three aspects of delay. Fig. 7(a1)–(a3) presented the results, revealing that manipulation patterns with no-delay factor had a significantly lower synergy ratio than those with a variable-delay factor. Among the motion patterns, push, pull, and SS showed higher synergy ratios compared with CR, CCR, PHCR, PLCR, PHCCR, and PLCCR. This indicates that CR, CCR, PHCR, PLCR, PHCCR, and PLCCR manipulations were less cooperative when operators maneuvered the robot to deliver the guidewire from the start point to target B. These manipulations also had larger delays compared with push, pull, and SS motions. This trend in synergy ratio also held true when considering the constant delay factor.

In Fig. 7(a3), single manipulation patterns, such as push, pull, CR, and CCR, generally had greater synergy ratios than compound manipulations, such as PHCR, PLCR, PHCCR, and PLCCR. This suggests that more complex manipulation patterns led to poorer cooperative performance between operators and the robot. Additionally, among the three different delay factors, the synergy ratio of manipulation patterns from group B was higher than those from groups A_A and A_B. This implies that the operator's manipulation behavior when delivering the guidewire influenced the control strategy of the primary–secondary robotic system, ultimately affecting the cooperative performance between operators and the robot.

Finally, the manipulation speed of each operator group was explored to understand the reasons behind the changes in cooperative performance with the robot in Table I. Fig. 8 showed significant differences in manipulation speeds among the three skill groups in the primary robot device. Operator B used slower speeds when pushing the guidewire compared with operators A_A and A_B. However, they used suitable speeds when pulling back the guidewire, falling between the fast speed of A_B and the slow speed of A_A. Operator A_A used quicker speeds when performing rotation manipulation to change the guidewire direction, indicating a lack of technical skill and cognition of manual PCI procedures, which could increase the risk of complications.

For complex vascular paths, operators needed to repeatedly deliver and withdraw compound manipulations to pass stenosis or branch sites. Operator B used higher speeds for PLCR, PHCCR, and PLCCR compound motions compared with operators A_A and A_B. However, they used slower speeds for PHCR when manipulating the guidewire through complex vascular pathways. This demonstrated that operator B used appropriate control strategies and technical skills based on their manual PCI experience from clinical practice.

Regarding the secondary device, it showed different manipulation speeds based on the operator group. For operator A_A, the manipulation speed of push and pull in the secondary device was similar to the corresponding manipulation speed in the primary device. However, the speeds for CR and CCR in the secondary device were lower than those in the primary device, indicating some difficulty for the secondary device to follow the primary manipulation, possibly leading to data loss. Additionally, for PHCCR and PLCCR motions, the manipulation speed of operator A_A in the secondary device was larger compared with the corresponding motion pattern in the primary device, suggesting that the secondary device rotated more randomly and did not seem to follow the primary's manipulation. On the other hand, for operators A_B and B, the manipulation speed of the primary device was similar to that of the secondary device, indicating better followability of the secondary device compared with operator A_A.

B. Analysis of Manipulation Time

Manipulation time of surgical procedure is commonly playing an important role in assessing a surgeon's technical skill [30]. For PCIs, the longer the manipulation time, the more the exposure to be suffered by both the patient and surgeon. First, the nonparameter independent test was applied to analyze the difference among different technical level groups on manipulation time

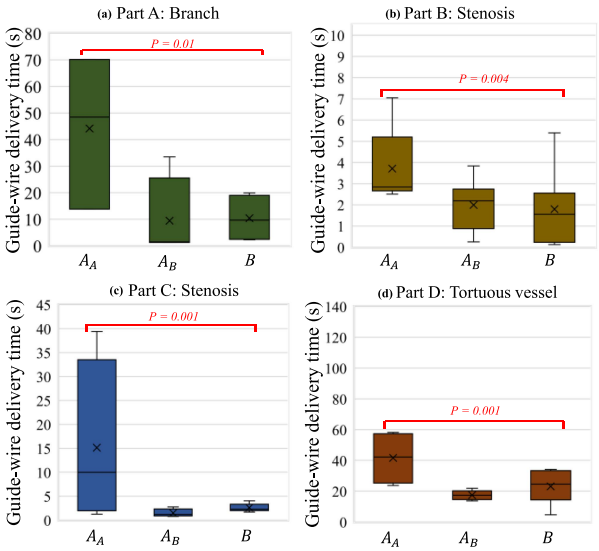

Fig. 9. Box figure shows time which different technical skill operators manipulated guidewire passing the (a) branch, (b) and (c) stenosis, and (d) tortuous vessel pathway. $p < 0.05$ denotes that there are significant differences in manipulation time among three groups.

of trial. The findings demonstrated a statistically significant difference ($p = 0.001$–0.01, $p < 0.05$) in manipulation times among the three different groups when operators maneuvered the guidewire through branch path A, stenosis paths B and C, and tortuous path D, respectively. Operator B took less time to complete the guidewire delivery in the paths with branch vessel (part A) and stenosis vessel (part B) compared with subjects A_A and A_B in Fig. 9(a) and (b); these results suggested that operator B has better performance and control strategy facing the branch A and stenosis B vessel pathway. Moreover, in stenosis vessel (part C) and tortuous vessel (part D), the manipulation time of operator B is slightly longer than that of subject A_B, and lower compared with operator A_A, which suggested that operator B existed some hesitantly consideration due to unfamiliarity with a robotic system. The manipulation time suggests that operator B with manual PCI experience shows different technical manipulations compared with operators A_A and A_B without PCI experience. When operator B manipulates the RCS for guidewire delivery in branch vessel, their technical skill and surgical cognition contribute to immediately change the manipulation strategy for ensuring the guidewire quickly pass through a complex pathway, they demonstrated fast learning curves. Whereas operators A_A and A_B without PCI experience lacked the control strategy and cognition for guidewire delivery. They used current cognition and knowledge to adjust their hand till the guidewire reached the target point.

C. Analysis of Distal and Contact Force

In order to investigate the interaction forces between operators and instruments, as well as tools and tissue during robot-assisted PCIs, the nonparametric Kruskal–Wallis ANOVA test was utilized. This test aimed to analyze the significant differences in operators' distal force and contact force among the three different groups when delivering the guidewire through branch, stent, and tortuous vessel pathways, as depicted in Figs. 10 and 11. The analysis of interaction information aimed to understand how operators with different technical skills adjust

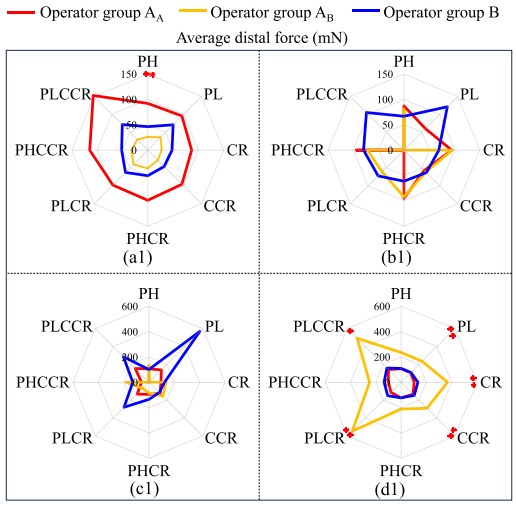

Fig. 10. Compared the average distal force among three groups A_A, A_B, and B, (a1) branch vessel A, (b1) stenosis vessel B, (c1) stenosis vessel C, and (d1) tortuous vessel D. $*$: significant difference ($*$: at 0.05 level and $**$: at 0.01 level).

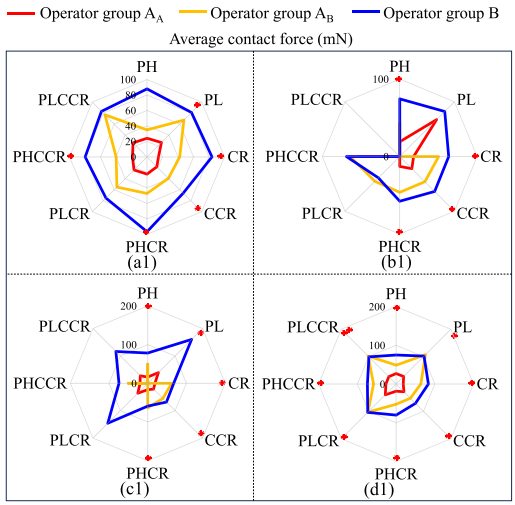

Fig. 11. Compared the average contact force among three skill groups, (a1) branch vessel A, (b1) stenosis vessel B, (c1) stenosis vessel C, and (d1) tortuous vessel D. $*$: significant difference ($*$: at 0.05 level and $**$: at 0.01 level).

their control strategies to prevent causing damage to vascular vessels through excessive force while ensuring enough tension to navigate through complex paths. This exploration provides valuable insights for designing haptic feedback systems tailored to operators with varying technical skill levels. Typically, this information is useful for selecting sensor material, precision, range, and stability. Effective component selection is also useful in evaluating the effectiveness of interactive forces during R-PCIs. It offers a way of reminding operators to either reduce or increase the operational forces to safely cannulate complex vascular paths.

1) Distal Force Between Instrument and Tissue: The generated intravascular force regarded as average distal force from operator A_A seems to be higher compared with the operator B passing branch vessel, as shown in Fig. 10(a1). This indicated that operator A_A did not know how to adjust the manipulation strategy to pass the branch vessel site safely and quickly during the robot-assisted catheterization. It is understood that higher

force between tools and tissue is easy to lead to the risk of vascular rupture. Likewise, operator B exhibited greater average distal force between the tools and tissue in comparison with operators A_A and A_B when delivering the guidewire through two stenotic sites. This observation implies that their manipulation strategy may involve providing enough tension to navigate through stenosis pathways effectively. Additionally, during the guidewire delivery through a tortuous vessel site in Fig. 10(d1), operator A_B applied a manipulation strategy that resulted in a higher average distal force between the guidewire and tissue compared with operators from groups A_A and B. The reason for this result could be that tortuous vessel pathway did not exist abnormal vascular, such as stenosis or branch site, operators did need to change the direction of guidewire and only along blood flow to push guidewire, as well operator A_B has more training experience than operators A_A and B on robot-assisted interventional procedure. In addition, manipulation strategy from operator B delivered guidewire passing through stenosis pathway C of 42.69%, which generated the higher average distal force between guidewire and tissue compared with that of passing through stenosis C path of 37.45%. This result suggested that the manipulation strategy needs to provide larger tension to pass through stenosis site, when operators deliver guidewire passing through the higher degree of stenosis pathway.

2) Contact Force Between Finger and Control Ring: A significant difference in average contact force between the finger and control ring was observed among the three groups of operators, as shown in Fig. 11. Specifically, operator B, who possesses manual PCI experience, displayed substantially higher average contact forces when performing PL (81.10 mN), CR (83.87 mN), CCR (66.07 mN), PHCR (96.58 mN), and PHCCR (79.87 mN) movements compared with the corresponding movements executed by operators A_A and A_B, who lacked prior PCI experience during the delivery of the guidewire through the branch vessel pathway [see Fig. 11(a1)]. Operator B with manual PCI experience is accustomed to directly holding the guidewire during manual PCI surgery, requiring a firm grip to prevent it from slipping. Consequently, when they handle the catheter and guidewire with a glove during robot-assisted PCI, the inherent gripping force developed through their manual PCI experience inadvertently influences the robot-assisted procedure.

Furthermore, the average contact force was lowest for operator A_A compared with the forces applied by operators A_B and B during the delivery of the guidewire through the vascular branch, stenosis, and tortuous pathways [see Fig. 11(a1)–(d1)]. This finding suggests that operator A_A lacked both the surgical cognition and control experience of interventional procedures and the experience of manipulating a robot. Consequently, they approached catheter/guidewire manipulation through each vascular path with caution to avoid vessel rupture or damage to the robot.

Moreover, the significant difference in performance of max/min distal force and contact force among three groups is shown in Appendix A (see Section IV–C and *Analysis* Figs. A4 and A5), respectively, while the significant difference of the distal force/contact force among the branch, stenotic, and tortuous vessel paths is further discussed in Appendix A (see Section IV–D *Comparison of operational…)*. This significant difference of distal force among four different vascular pathways based on operators A_A, A_B, and B demonstrated that manipulating of delivery guidewire passing through branch, stenosis, and tortuous pathway uses different control strategies to avoid vascular rupture for three group operators, respectively.

V. Evaluation Model and Interaction Information

Manual PCIs involve direct tool manipulation using a surgeon's hand, whereas robot-assisted PCI surgery is performed by operating the primary robotic device, with the secondary device replicating the operator's motion control instructions to manipulate the interventional tools. Therefore, the level of cooperation between the operator and the robot has a significant impact on the stability and safety of the robot-assisted PCI procedure. In a primary–secondary isomorphic robotic system, delays can affect the real-time interaction between operators and the primary–secondary mechanism, leading to a reduction in the overall system control. Poor cooperation between operators and the robot can significantly decrease the surgical robotic stability and effectiveness, posing risks and challenges to the smooth implementation of the PCI procedure.

Some existing studies suggested that the imprecise motion control, communication delay, and the application of excessive force also contribute to inefficient proximal-to-distal transmissions [31], [32]. Despite the assertion, only a few studies have been done to explore the contribution of the delay factors based on haptic force, manipulating speed, and technical skills utilized for robot-assisted cardiovascular interventions. In this study, we conducted a 3-D vascular simulator experiment to investigate the cooperative performance between operators with varying technical skills and the robot. We focused on three aspects of delay consideration and analyzed the distal force between tools and tissue, as well as the contact force between fingers and the control ring during robot-assisted interventions.

Multimodal datasets, including muscle activity and finger motion information from operators, contact force between operator–control-ring contact, proximal force between tool–mechanism contact, distal force between tools–tissue contact, and position and rotation information from primary–secondary system, were acquired with wearable sensor technologies to assess cooperative performance between operator and robot during a robot-assisted catheter procedure. Multiple data sources were applied to develop predictive evaluation framework based on manipulation pattern for cooperative performance between operators and robot analysis. The model on recognizing different manipulation patterns shows good performance of the training and validation dataset, while the proposed network model also demonstrated a better recognition accuracy on test dataset, as shown in Fig. 6. The results suggested that the proposed evaluation framework provided a reliability and effectiveness on further capturing the synergy ratio.

The structural design of the primary–secondary isomorphic robot system inherently introduces a delay factor. When this delay remains within an acceptable range, the system can be considered as satisfied or extremely satisfied [33]. Initially, we assumed the current system without any delay or with minimal delay and explored the cooperative performance between operators and the robot. The results revealed a low synergy ratio between operators and the robotic system for all three groups of operators, indicating that the robotic secondary device might not be able to repeat operators' manipulations in real time due to the impact of a delay factor. Therefore, we took into consideration the communication-delay factor of the entire robotic system, which was treated as a constant delay factor.

The results showed a slight increase in the synergy ratio between operators and the robot, suggesting that this constant delay factor accounted for only a portion of the overall delay, while other factors contributing to the delay were not fully captured. When considering a variable-delay factor based on manipulation, the results showed higher synergy ratios between operators and the robot compared with the other two delay factor considerations. Additionally, operator B exhibited higher synergy ratios compared with operators A_A and A_B. These results, considering the three aspects of delay factor, indicated that different operating behaviors could impact the coordination of human–machine control strategies in the primary–secondary robotic system.

Using manipulation-based delay factors, where motion patterns are treated as units to determine delay times, proved to be more effective in accounting for the impact of delay caused by packet loss conditions based on a time scale. This is because, with manipulation-based delay factors, even if there is a short-term packet loss, it does not disrupt the state of the entire manipulation pattern, as it would if time-based units were used. This makes manipulation-based delay factors more suitable for application in the primary–secondary isomorphic robotic system.

Furthermore, temporal metrics often exhibit correlations with the skill level [34]. The results obtained from the manipulation time and speed of each motion pattern also confirmed that operators with different technical skills applied different manipulation strategies. Their varying technical skills, including surgical cognition, control strategy usage, manipulating speed, contact force, behavior patterns, and control strategies, all contributed to the cooperative performance between operators and the robot. The promising outcomes of this study demonstrate that the proposed evaluation framework holds great potential for assessing the cooperative performance between operators and the robot. Additionally, the use of manipulation-based variable-delay factors contributes to designing better control strategies and provides a reference for improving the cooperative performance between operators and the robotic system.

Moreover, in R-PCI surgery, the key factor is to manipulate the robotic system such that the catheter/guidewire is delivered to the target safely and timely. It is normal that experts have more precise control technical skills than novices could have in cardiac interventional surgery, but it is unknown for R-PCI surgery, whether their technical skill, which manipulates robot delivery guidewire, is better than operators without PCI experience. The robot-assisted procedures were statistically analyzed with respect to the manipulating time, the distal force between tools and tissues, and contact force between fingers and control ring. The data were obtained to characterize the technical skills when navigating through the branched, stenotic, and tortuous vessels. According to manipulating time, the result observed that operator B with PCI experience took shorter time passing through branch A, stenosis B, stenosis C, and tortuous D path compared with operator A_A without PCI experience, while operator B spent slightly longer time passing through stenosis C and tortuous D path compared with operator A_B without PCI experience (see Fig. 9). These results showed that operator B exhibited superior technical skills in comparison with operators without prior experience in PCI during the robot-assisted PCI procedure. This superiority was attributed to their extensive knowledge of surgical techniques and effective strategies for navigating complex vascular pathways, which they had gained through their previous experience in manual PCI surgeries.

Ultimately, the aim was to investigate how operators with varying technical skills adjust their control strategies to avoid causing damage to vascular vessels through excessive force while maintaining sufficient tension to navigate complex pathways. The analysis involved evaluating the distal force between tools and tissues and the contact force between fingers and the control ring, based on the expertise levels of the operators. The statistical analysis employed the nonparametric Kruskal–Wallis ANOVA test, where significant differences were denoted with asterisks (* indicating $p < 0.05$ and ** indicating $p < 0.01$). This approach allowed us to uncover valuable insights into how operator skill impacts the delicate balance between applying appropriate force and ensuring safe navigation during the procedure. The results obtained showed significant difference when the operators catheterized through the branched, stenotic, and tortuous vessel pathways. When operator A_A delivers the guidewire through the branched path, a larger distal force between tools and tissues (average 100 mN) was observed than the other operators A_B and B (A_B with 25 mN and B with 50 mN). Although the contact force between finger and control ring recorded for the operator A_A was small (average 20 mN), their manipulating speeds were faster than the other two groups, especially for rotation operations. This could lead to larger distal interaction force. Operator A_A does not know how to adjust manipulating behavior to pass through the branch pathway due to lack of control strategy and cognition experience of surgery for complex vessel pathway, which could enhance the risk of vessel rupture. Moreover, operator B used a larger contact force to manipulate control ring, and the distal interaction force is small passing through branch and tortuous vessel pathway, respectively. These show that such an operator B could transfer their manipulation strategy and cognition of M-PCI experience to manipulate the guidewire robotically during R-PCIs. In M-PCI procedures, operator uses a large contact force to sense the interaction force of the intravascular catheter/guidewire and avoids accidental shedding of catheter/guidewire from hand due to small haptic force.

In the meantime, it was observed that when a larger contact force was applied to deliver the guidewire through stenotic paths, the distal force also increased (with an average of 100 mN). This larger force was necessary to ensure sufficient tension for navigating through the narrowed pathway and avoiding any potential obstacles that might hinder the passage. This finding aligns with the outcomes of our previous research [21]. Furthermore, the study revealed significant differences in the distal force between the tool and tissue, as well as the contact force between the operator's finger and the control ring, among the different pathways (branch A, stenosis B, stenosis C, and tortuous D) across the three operator groups. These variations indicate that specific pathways demand distinct manipulation strategies from the operators to safely navigate through complex vessels during robot-assisted interventional procedures. Considering these outcomes, it becomes intriguing to devise a numerical representation that allows operators to forecast the state of the vascular pathway (branch, stenosis, and tortuous path) beforehand. Such information would serve as a valuable guide, enabling operators to adapt their manipulation strategies promptly, thereby reducing the risk of vascular rupture during future procedures.

VI. Conclusion and Future Works

This study presents the development of a manipulation-based framework designed to assess cooperative performance between operators with varying technical skills and a robot in a 3-D vascular simulator during robot-assisted interventional procedures. The framework integrates multiple data sources, including operators' MAs, finger motion, contact force between fingers and control ring, distal forces between tools and tissues, proximal force between tool instruments and tissues, as well as position and rotation information from both primary and secondary devices in the RCS during robot-assisted intravascular catheterization. Through training, validation, and testing datasets, this framework proves to be reliable and effective in calculating the synergy ratio. The investigation considers three aspects of delay factors: no delay, constant delay, and variable delay. Particularly, the manipulation-based variable-delay factor holds great potential for enhancing cooperative performance between operators and the robot. This potential improvement can lead to more seamless and efficient collaboration during procedures. Additionally, the study delves into analyzing the distal force between catheter/guidewire–tissue and the contact force between fingers and the control ring. The aim is to understand how operators with different technical skills adjust their control strategies to avoid damaging vascular vessels due to excessive force while still providing sufficient tension to navigate complex pathways. This knowledge is valuable for guiding sensor selection and designing haptic feedback systems with the appropriate perceived resolution. In future work, the study plans to fine-tune delay parameters to achieve adaptability for real-time human–machine robotic systems, all while maintaining an acceptable safety profile. This will facilitate the application of the framework in actual medical settings, further advancing the field of robot-assisted interventions.

References

[1] A. Timmis et al., "European society of cardiology: Cardiovascular disease statistics 2019," *Eur. Heart J.*, vol. 41, no. 1, pp. 12–85, 2020.

[2] S. Ojeda, R. Romaguera, I. Cruz-Gonzalez, and R. Moreno, "Spanish cardiac catheterization and coronary intervention registry: 29th official report of the interventional cardiology association of the Spanish Society of Cardiology (1990-2019)," *Revista Espanola de Caradiologia*, vol. 73, no. 11, pp. 927–936, 2020.

[3] E. Mahmud et al., "Demonstration of the safety and feasibility of robotically assisted percutaneous coronary intervention in complex coronary lesions: Results of the CORA-PCI study," *JACC, Cardiovasc. Interv.*, vol. 10, pp. 1320–1327, 2017.

[4] E. J. Benjamin et al., "Heart disease and stroke statistics-2017 update: A report from the American Heart Association," *Circulation*, vol. 135, no. 10, pp. e146–e603, 2017.

[5] H. Su et al., "State of the art and future opportunities in MRI-guided robot-assisted surgery and interventions," *Proc. IEEE*, vol. 110, no. 7, pp. 968–992, Jul. 2022.

[6] A. Khamis et al., "Robotics and intelligent systems against a pandemic," *Acta Polytechnica Hungarica*, vol. 18, no. 5, pp. 13–35, 2021.

[7] K. C. Sajja et al., "Endovascular robotic: Feasibility and proof of principle for diagnostic cerebral angiography and carotid artery stenting," *J. Neurointerventional Surg.*, vol. 12, no. 4, pp. 345–349, 2020.

[8] C. Beaman, H. Saber, and S. Tateshima, "A technical guide to robotic catheter angiography with the corindus CorPath GRX system," *J. Neurointerventional Surg.*, vol. 14, 2022, Art. no. 1284.

[9] Y. Zhao et al., "Remote vascular interventional surgery robotics: A literature review," *Quantitative Imag. Med. Surg.*, vol. 12, no. 4, pp. 2552–2574, 2022.

[10] G. Fichtinger, J. Troccaz, and T. Haidegger, "Image-guided interventional robotics: Lost in translation?," *Proc. IEEE*, vol. 110, no. 7, pp. 932–950, Jul. 2022.

[11] F. Picard et al., "The ongoing saga of the evolution of percutaneous coronary intervention: From balloon angioplasty to recent innovations to future prospects," *Can. J. Cardiol.*, vol. 38, no. 10, pp. S30–S41, 2022.

[12] A. Saikia and S. M. Hazarika, "cBDI: Towards an architecture for human-machine collaboration," *Int. J. Social Robot.*, vol. 9, no. 2, pp. 211–230, 2016.

[13] A. Smirnov and A. Ponomarev, "Human-machine collective intelligence environment for decision support: Conceptual and technological design," in *Proc. 27th IEEE Conf. Open Innov. Assoc.*, 2020, pp. 253–259.

[14] O. Kostyukova, F. P. Vista IV, and K. T. Chong, "Design of feedforward and feedback position control for passive bilateral teleoperation with delays," *ISA Trans.*, vol. 85, pp. 200–213, 2019.

[15] S. Zhai and J. Senders, "Investigating coordination in multidegree of freedom control II: Correlation analysis in 6 DOF tracking," in *Proc. 41st Conf. Hum. Factors Ergonom. Soc. Annu. Meeting*, 1997, vol. 1–2, pp. 1254–1258.

[16] N. Xi, T.-J. Tarn, and A. K. Bejczy, "Intelligent planning and control for multirobot coordination: An event-based approach," *IEEE Trans. Robot. Autom.*, vol. 12, no. 3, pp. 439–452, Jun. 1996.

[17] A. E. Sklar and N. B. Sarter, "Good vibrations: Tactile feedback in support of attention allocation and human-automation coordination in event-driven domains," *Hum. Factors*, vol. 41, no. 4, pp. 543–552, 1999.

[18] K. Huang, D. Chitrakar, R. Mitra, D. Subedi, and Y.-H. Su, "Characterizing limits of vision-based force feedback in simulated surgical tool-tissue interaction," in *Proc. 42nd Annu. Int. Conf. IEEE Eng. Med. Biol. Soc.*, 2020, pp. 4903–4908.

[19] C. E. Reiley and G. D. Hager, "Task versus subtask surgical skill evaluation of robotic minimally invasive surgery," in *Proc. Med. Image Comput. Comput.-Assist. Intervention*, 2009, pp. 435–442.

[20] X.-H. Zhou, G.-B. Bian, X.-L. Xie, Z.-G. Hou, R.-Q. Li, and Y.-J. Zhou, "Qualitative and quantitative assessment of technical skills in percutaneous coronary intervention: In vivo porcine studies," *IEEE Trans. Biomed. Eng.*, vol. 67, no. 2, pp. 353–364, Feb. 2020.

[21] W. Du et al., "Exploration of interventionists' technical manipulation skills for robot-assisted intravascular PCI catheterization," *IEEE Access*, vol. 8, pp. 53750–53765, 2020.

[22] R. V. Patel, S. F. Atashzar, and M. Tavakoli, "Haptic feedback and force-based teleoperation in surgical robotics," *Proc. IEEE*, vol. 110, no. 7, pp. 1012–1027, Jul. 2022.

[23] Q. Gao, J. Wu, Y. Song, J. Liu, Z. Mao, and Y. Zhan, "A novel contact force measurement scheme for slave catheter robot in robotic endovascular surgery," in *Proc. IEEE Int. Conf. Mechatron. Autom.*, 2021, pp. 164–169.

[24] L. Gan, W. Duan, T. O. Akinyemi, W. Du, O. M. Omisore, and L. Wang, "Development of a fiber Bragg grating-based force sensor for minimally invasive surgery—Case study of ex-vivo tissue palpation," *IEEE Trans. Instrum. Meas.*, vol. 72, Dec. 2023, Art. no. 4010012.

[25] W. Du et al., "Exploring operators' natural behaviors to predict catheterization trial outcomes in robot-assisted intravascular interventions," *IEEE Trans. Med. Robot. Bionics*, vol. 4, no. 3, pp. 682–695, Aug. 2022.

[26] O. M. Omisore et al., "Weighting-based deep ensemble learning for recognition of interventionalists' hand motions during robot-assisted intravascular catheterization," *IEEE Trans. Hum. Mach. Syst.*, vol. 53, no. 1, pp. 215–227, Feb. 2023.

[27] O. M. Omisore et al., "Automatic tool segmentation and tracking during robotic intravascular catheterization for cardiac interventions," *Quantitative Imag. Med. Surg.*, vol. 11, no. 6, pp. 2688–2710, 2021.

[28] N. Werner, G. Nickenig, and J.-M. Sinning, "Complex PCI procedures: Challenges for the interventional cardiologist," *Clin. Res. Cardiol.*, vol. 107, no. 2, pp. S64–S73, 2018.

[29] T. O. Akinyemi et al., "Adapting neural-based models for position error compensation in robotic catheter systems," *Appl. Sci.*, vol. 12, 2022, Art. no. 10936.

[30] R. N. Elek and T. Haidegger, "Robot-assisted minimally invasive surgical skill assessment—Manual and automated platforms," *Acta Polytechnica Hungarica*, vol. 16, no. 8, pp. 141–169, 2019.

[31] A. Takacs, I. J. Rudas, R.-E. Precup, L. Kovacs, and T. Haidegger, "Models for force control in telesurgical robot systems," *Acta Polytechnica Hungarica*, vol. 12, no. 8, pp. 95–114, 2015.

[32] J. Inga et al., "Human-machine symbiosis: A multivariate perspective for physically coupled human-machine systems," *Int. J. Human-Comput. Stud.*, vol. 170, 2023, Art. no. 102926.

[33] T. M. Patela, S. C. Shah, and S. B. Pancholy, "Long distance tele-robotic-assisted percutaneous coronary intervention: A report of first-in-human experience," *EClinicalMedicine*, vol. 14, pp. 53–58, 2019.

[34] T. D. Nagy and T. Haidegger, "Performance and capability assessment in surgical subtask automation," *Sensors*, vol. 22, no. 7, 2022, Art. no. 2501.